

# SCIENTIFIC REPORTS



OPEN

## Diabetic cornea wounds produce significantly weaker electric signals that may contribute to impaired healing

Received: 14 January 2016

Accepted: 04 May 2016

Published: 10 June 2016

Yunyun Shen<sup>1,2</sup>, Trisha Pfluger<sup>1</sup>, Fernando Ferreira<sup>1,3</sup>, Jiebing Liang<sup>4</sup>, Manuel F. Navedo<sup>5</sup>, Qunli Zeng<sup>2</sup>, Brian Reid<sup>1</sup> & Min Zhao<sup>1,6</sup>

Wounds naturally produce electric signals which serve as powerful cues that stimulate and guide cell migration during wound healing. In diabetic patients, impaired wound healing is one of the most challenging complications in diabetes management. A fundamental gap in knowledge is whether diabetic wounds have abnormal electric signaling. Here we used a vibrating probe to demonstrate that diabetic corneas produced significantly weaker wound electric signals than the normal cornea. This was confirmed in three independent animal models of diabetes: db/db, streptozotocin-induced and mice fed a high-fat diet. Spatial measurements illustrated that diabetic cornea wound currents at the wound edge but not wound center were significantly weaker than normal. Time lapse measurements revealed that the electric currents at diabetic corneas lost the normal rising and plateau phases. The abnormal electric signals correlated significantly with impaired wound healing. Immunostaining suggested lower expression of chloride channel 2 and cystic fibrosis transmembrane regulator in diabetic corneal epithelium. Acute high glucose exposure significantly (albeit moderately) reduced electrotaxis of human corneal epithelial cells *in vitro*, but did not affect the electric currents at cornea wounds. These data suggest that weaker wound electric signals and impaired electrotaxis may contribute to the impaired wound healing in diabetes.

Delayed or non-healing wounds pose an immense health and economic problem, affecting the quality of life of millions of patients globally. The World Health Organization estimated that the global prevalence of diabetes in 2014 was 9% and that it will be the 7<sup>th</sup> leading cause of death in 2030<sup>1</sup>. Impaired wound healing in diabetic patients results in adverse pathological changes such as chronic foot ulceration which affects approximately 15% of diabetic patients<sup>2</sup>. This burden is growing rapidly due to increasing health care costs, an aging population, and a sharp rise in the incidence of diabetes and obesity worldwide<sup>3,4</sup>. Diabetic patients may also suffer from corneal recurrent erosions/ulcerations<sup>5</sup> which are difficult to treat and may result in significant ocular morbidity and visual impairment<sup>6,7</sup>. The mechanisms underlying wound healing defects in diabetic patients are not fully understood, but may include deregulation of the biochemical milieu such as microcirculatory changes, altered growth factors, abnormal cytokine production, genetic or epigenetic changes and inflammatory state<sup>8,9</sup>.

Electric fields (EFs) occur naturally at wounds<sup>10</sup>. The corneal epithelium actively generates and maintains an electrical trans epithelial potential (TEP)<sup>11</sup> by active directional pumping of ions between the stroma and tear side<sup>12</sup>. Wounding collapses the local TEP resulting in significant electric potentials and currents between the wound and the surrounding intact epithelium, establishing the cathode at the wound<sup>13</sup>. The existence of these endogenous wound electric currents has been confirmed using different modern techniques<sup>14–16</sup>. We use “electric signals” to denote steady, direct-current EFs that are intrinsically associated with steady fluxes of ions.

<sup>1</sup>Department of Dermatology, University of California, Davis, CA, USA. <sup>2</sup>Bioelectromagnetics Laboratory, Department of Occupational and Environmental Health, School of Public Health, School of Medicine, Zhejiang University, Hangzhou, China. <sup>3</sup>Department of Biology, Centre of Molecular and Environmental Biology (CBMA), University of Minho, Braga, Portugal. <sup>4</sup>Department of Biology, California State University, Northridge, CA, USA. <sup>5</sup>Department of Pharmacology, University of California, Davis, CA, USA. <sup>6</sup>Department of Ophthalmology and Vision Science, University of California, Davis, CA, USA. Correspondence and requests for materials should be addressed to M.Z. (email: minzhao@ucdavis.edu)

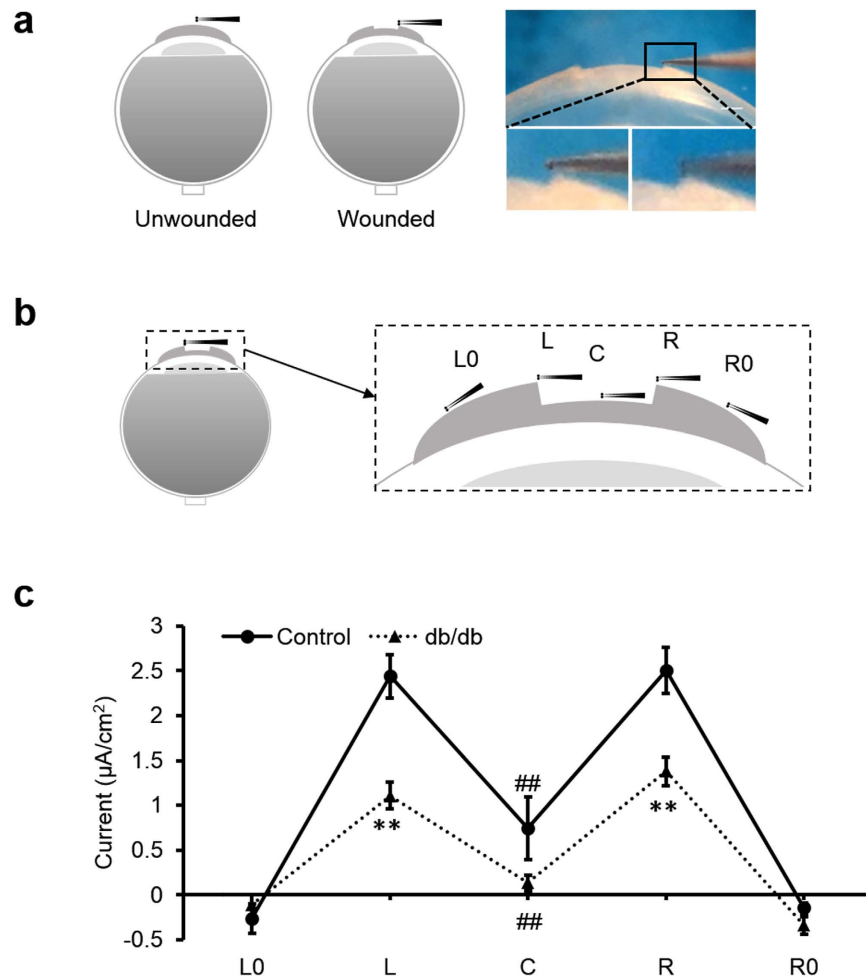


**Figure 1. Diabetic corneas generated significantly weaker wound electric signal.** (a) Schematic diagram of the wound current measurement with the probe positioned at the unwounded center and wound edge. Photographs on the right show the probe in measuring position at the right wound edge. The close-ups below show the probe without vibration for clarity (left) and the probe vibrating (blurred double image) on the right. Scale bar: 250  $\mu\text{m}$ . (b) Positions of the vibrating probe when measuring electric current at different places across the wounded cornea: left unwounded position (L0), left wound edge (L), wound center (C), right wound edge (R) and right unwounded position (R0). (c) Electric current profile of wounded control and db/db diabetic corneas. Positive values are outward current (flow of positive charge), negative values are inward. Currents were significantly greater at the wound edges than at the wound center ( $p < 0.01$ ; Student t-test). Currents at the wound edge of diabetic cornea were significantly weaker than in the control group (\*\* $p < 0.01$ ). Currents at the wound center were not significantly different (##NS). Interestingly, currents at the unwounded cornea outside the wound were on average slightly inward. Data are mean  $\pm$  S.E.M. from 4 independent wounds.

Wound repair is a precise and complex process necessary to recover tissue function after injury. Effective wound healing requires tightly controlled cell movement and tissue growth<sup>17</sup>. Epithelial cells, including corneal epithelial cells (CECs) and skin keratinocytes, respond robustly by directional migration in EFs of strengths that have been measured at wounds *in vivo*<sup>18,19</sup>. The EFs override co-existing directional signals such as free edge and contact inhibition release. Migration of CECs is guided by EFs of physiological strength when applied in a direction opposite to other cues<sup>20</sup>. Applied EFs as low as 12.5 mV/mm guide migration of CECs to the cathode, the same direction of the wound EFs<sup>18</sup>. Electrical stimulation has been approved in the U.S. for treatment of refractory chronic wounds in patients (chronic Stage III or Stage IV pressure ulcers, arterial ulcers, diabetic ulcers and venous stasis ulcers), because of apparent clinical benefits<sup>21–23</sup>.

It is, however, not known whether diabetic wounds have abnormal electric signals. Here we tested the hypothesis that diabetic corneas produce weaker electrical signals compared to normal corneas and that the weaker signals may contribute to the impaired wound healing. We also tested whether high glucose affects directional cell migration guided by small-applied electric fields.

## Results

**Diabetic cornea wounds lost the large electric signal.** We used a vibrating probe to measure the intact and wounded cornea electric current (Fig. 1a). To profile the cornea wound current, five different positions inside

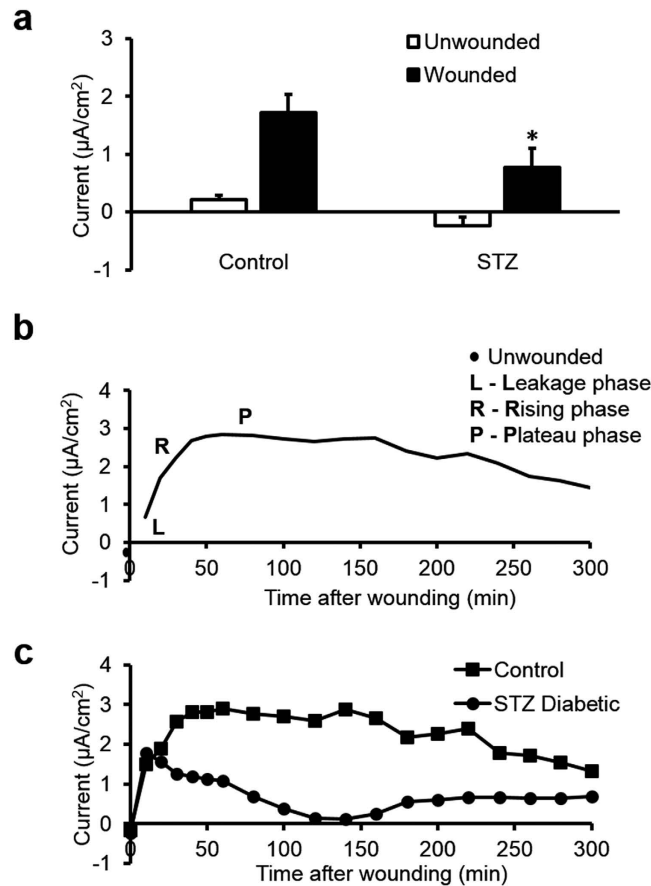


**Figure 2. Streptozotocin (STZ) induced diabetic cornea wounds showed an impaired wound electric signal and lost the putative active transport phases.** (a) STZ diabetic cornea wounds had significantly smaller electric signals. White bars are unwounded current and black bars are wound edge current. Data are mean  $\pm$  S.E.M. from 6 independent wounds. Control: age-matched vehicle-injected controls. \* $p < 0.05$ , when compared with the control value, Student  $t$ -test. (b) Three phases of the naturally-occurring electric currents at mouse cornea wound recorded in the hours after wounding. Line is a best fit (rolling average, two period) of the mean control mouse electric current time lapse data. (c) Time lapse wound currents in control and diabetic mice measured for five hours after wounding. STZ diabetic cornea lost the rising and plateau phases. Squares are age-matched vehicle-injected control and circles are STZ-induced diabetic.

and outside the wound were measured with the vibrating probe 40 min post-wounding, as this is the approximate time the current reaches maximum (Fig. 1b). In control corneas, currents were maximal at the wound edges and smaller at the wound center (Fig. 1c). Diabetic db/db cornea wounds showed a similar profile: the wound current at the edges were three times larger than that at the wound center ( $n = 4$ ,  $p < 0.01$ ). Currents at the wound center were not significantly different ( $n = 4$ ,  $p > 0.05$ ). However, diabetic cornea wound currents at both the right and left edges displayed significantly weaker electric signals than the control group ( $n = 4$ ,  $p < 0.01$ ). We confirmed this result in a different diabetes model, streptozotocin (STZ)-injected. STZ-induced diabetic cornea wound edges also showed significantly weaker electric signals (Fig. 2a) ( $n = 6$ ,  $p < 0.05$ ).

These wound profile data support our previous hypothesis that the wound edge current depends more on active transport whereas the smaller current at the wound center may be more due to ion leakage<sup>24</sup>. These spatial maps also suggest that the stroma at the wound center does not generate significant ion flux and that diabetic corneas have less active (translocator-mediated) ion flux than control ones. Interestingly, currents outside the wounds were slightly inward, suggesting a circuit of current flowing outward at the wound and inward in the surrounding intact corneal epithelium.

**Diabetic cornea wound current lost the rising and plateau phases in the timelapse measurements.** We next recorded the time course of the wound electrical signals in control and STZ-induced diabetics. In normal age-matched saline-injected control mice, cornea electric currents showed characteristic dynamic changes after wounding: leakage phase (L), rising phase (R) and plateau phase (P) (Fig. 2b). Electric currents at cornea wounds from STZ-induced diabetic mice lacked these characteristic rising and plateau phases (Fig. 2c). This suggests that ion channels and pumps which generate the cornea electric signals (e.g., TEP and associated wound fields and currents) might be downregulated in diabetes.

We also used the vibrating probe to measure electric current time-course in different diabetes models: db/db and high-fat diet (HFD) diabetic mice. Blood glucose levels were measured before the vibrating probe

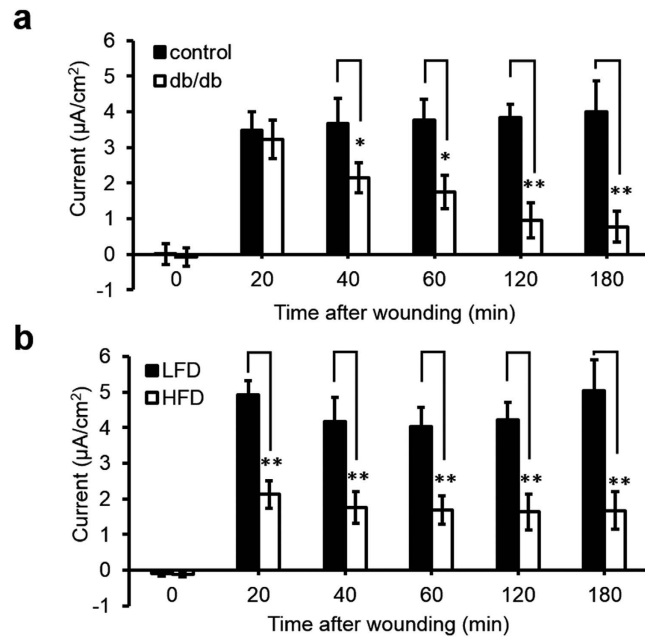


**Figure 3. A genetic knockout model of diabetes in mice (db/db) and high-fat diet (HFD) diabetic mice also showed a weaker electric signal at the cornea wound.** (a) Diabetic db/db cornea wounds generated weaker electric signals. Black bars are the age-matched heterozygous genetic control group and white bars are the diabetic db/db group,  $n = 6$ . (b) Weaker electric current was also observed in high-fat diet induced diabetic mouse cornea wounds. Black bars are age-matched low fat diet control group (LFD) and white bars are high-fat diet induced diabetic group (HFD),  $n = 4$ . Data are mean  $\pm$  S.E.M. \* $p < 0.05$ , \*\* $p < 0.01$ , when compared with the matched control value, Student  $t$ -test.

measurement to confirm the diabetic status (Table S1). After wounding, db/db corneas generated weaker currents compared to the age-matched control group ( $n = 6$ ,  $p < 0.05$ ) (Fig. 3a). Three hours after wounding, the currents at cornea wounds of control mice remained significantly larger ( $4.01 \pm 0.86 \mu\text{A}/\text{cm}^2$ ), more than five times larger than in the db/db mice ( $0.77 \pm 0.44 \mu\text{A}/\text{cm}^2$ ) ( $n = 6$ ,  $p < 0.01$ ). Consistently, electric currents at cornea wounds in HFD mice were also significantly smaller than the controls. Electric signal decreased significantly at cornea wounds in HFD-induced mice at 20 min post-wounding and thereafter for up to 3 h ( $n = 4$ ,  $p < 0.01$ ) (Fig. 3b).

Interestingly, 1 out of 6 corneas of db/db diabetes, 2 out of 6 corneas of STZ-induced diabetes and 1 out of 4 corneas of HFD mice had inward wound currents. This was unusual and was never seen in any cornea wound in healthy wild-type mouse, rat or human<sup>25,26</sup>, which always show outward cornea wound currents.

Diabetic patients can often have abnormally high levels of glucose in their tears<sup>27</sup>. We tested whether high glucose in the bathing solution altered the cornea wound electric signal. Corneas pre-incubated in high glucose (30 mM) for 3 h prior to wounding did not show significantly different electric currents (unwounded or wounded) when compared with control eyes incubated in normal glucose (5.6 mM) for the same time (Fig. S1). Therefore, diverse diabetes models consistently have weaker cornea wound electric signals compared to matched controls, and it cannot be mimicked by acute exposure to high glucose.

**Diabetic cornea wound healing rate correlated with the wound currents.** To quantify cornea wound healing, we made similar-sized epithelial wounds in control and diabetic mice ( $\Phi \sim 1.4$  mm) and visualized the wound with fluorescein dye. Wound areas were not significantly different at time zero ( $p > 0.5$ ). Cornea wounds in control mice healed quickly: at 24 h they were more than 50% healed ( $< 1/2$  original area), and by 48 h were almost completely healed (Fig. 4a,b). In contrast, STZ-treated mice wounds healed slowly. There was no healing in the first 24 h and by 48 h they had healed an average of only 42.6% ( $p < 0.05$ ) (Fig. 4a,b). HFD and db/db mice corneas also healed much slower than age-matched control corneas ( $p < 0.01$ ) (Fig. 4a,b).

We used the Pearson correlation analysis to determine the relationship between impaired wound healing and the wound electric currents. The analysis showed that the wound healing rate correlated significantly with the changes in wound electric current (Fig. 4c). Results from two different diabetic mouse models showed a positive correlation between wound current and wound healing. Thus, eyes with small (or even inward) currents showed poor wound healing whereas eyes with larger currents showed better wound healing. Paired analyses of db/db mice (Pearson correlation coefficient,  $R = 0.990$ ) and HFD mice (Pearson correlation coefficient,  $R = 0.987$ ) showed significant correlation ( $n = 4$ ,  $p = 0.010$  and  $n = 4$ ,  $p = 0.013$ , respectively) (Fig. 4c).

**Decreased expression of CFTR and CLC2 in diabetic corneal epithelium.** To test possible changes in ion translocators in diabetic corneas we labeled chloride channel 2 (CLC2) and cystic fibrosis transmembrane conductance regulator (CFTR) because these channels are expressed in corneal epithelium and  $\text{Cl}^-$  fluxes were

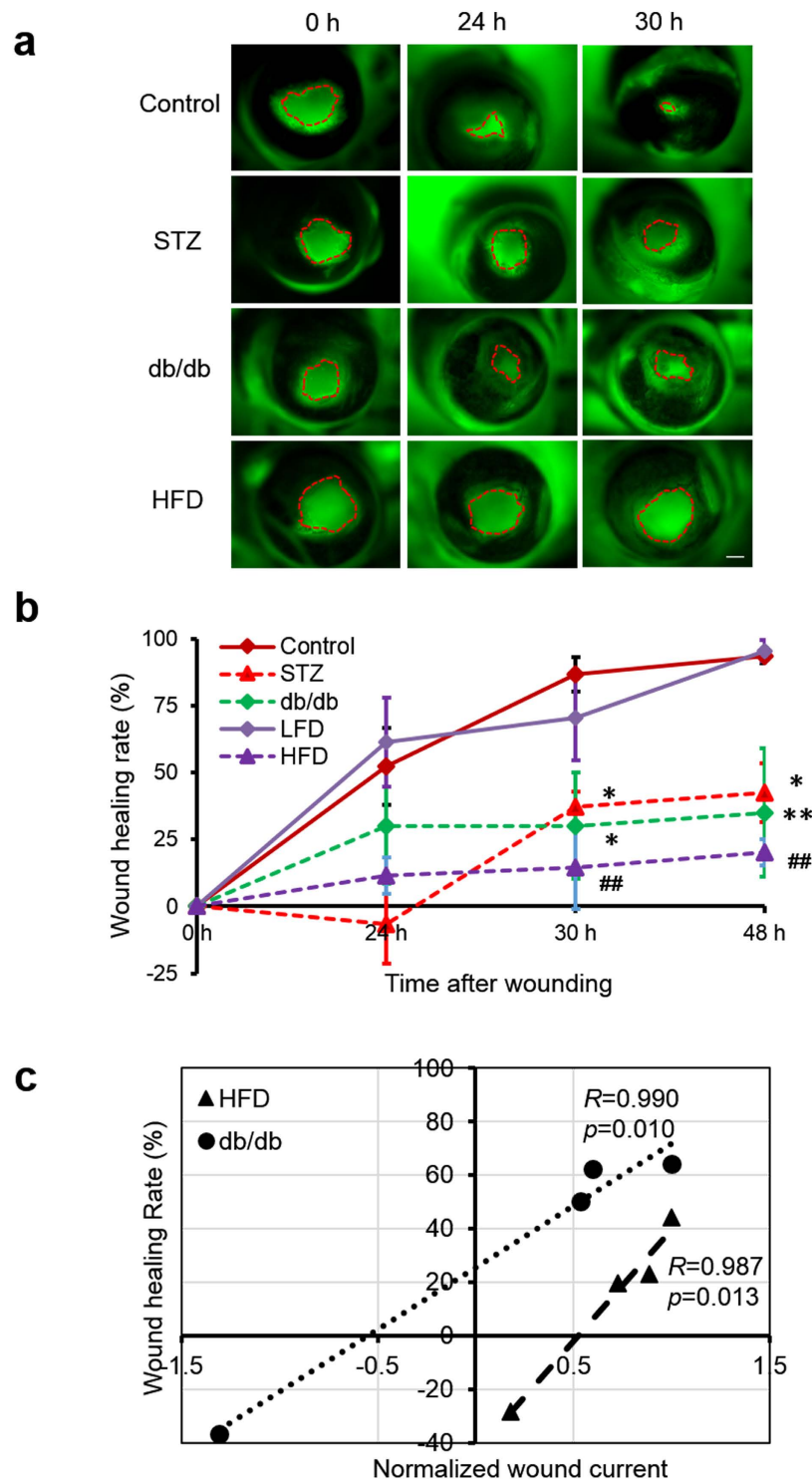


**Figure 4. Impaired wound healing in diabetic corneas was correlated significantly with weak wound electric currents.** (a) Diabetic cornea wounds in three different mouse diabetes models showed significantly slower wound healing than control wounds. Wound areas were not significantly different at time zero ( $p > 0.5$ ). Scale bar:  $500\mu\text{m}$ . (b) Healing rate of cornea wounds in control and diabetic mice. Age-matched control and low fat diet (LFD) wounds (solid lines) healed almost 100% in 48 h. All three diabetic models (dashed lines) healed significantly slower. Values are mean  $\pm$  S.E.M. from 4 or more independent experiments, \* $p < 0.05$ , \*\* $p < 0.01$ , when compared with the control value, ## $p < 0.01$ , when compared with low fat diet (LFD) group, Student  $t$ -test. (c) Data from each eye were plotted as wound current vs wound healing and the Pearson correlation coefficient calculated. Significant correlation was seen between wound current and wound healing (in paired data) from db/db and high-fat diet (HFD) diabetic mice. Each set of data (HFD and db/db) were normalized so that their maximum wound current was  $1\mu\text{A}/\text{cm}^2$ , so they could be plotted on the same chart. Pearson correlation coefficient ( $R$ ) and significance value ( $p$ ) value are as shown. db/db,  $R = 0.990$ ,  $p = 0.010$ ; HFD,  $R = 0.987$ ,  $p = 0.013$ .

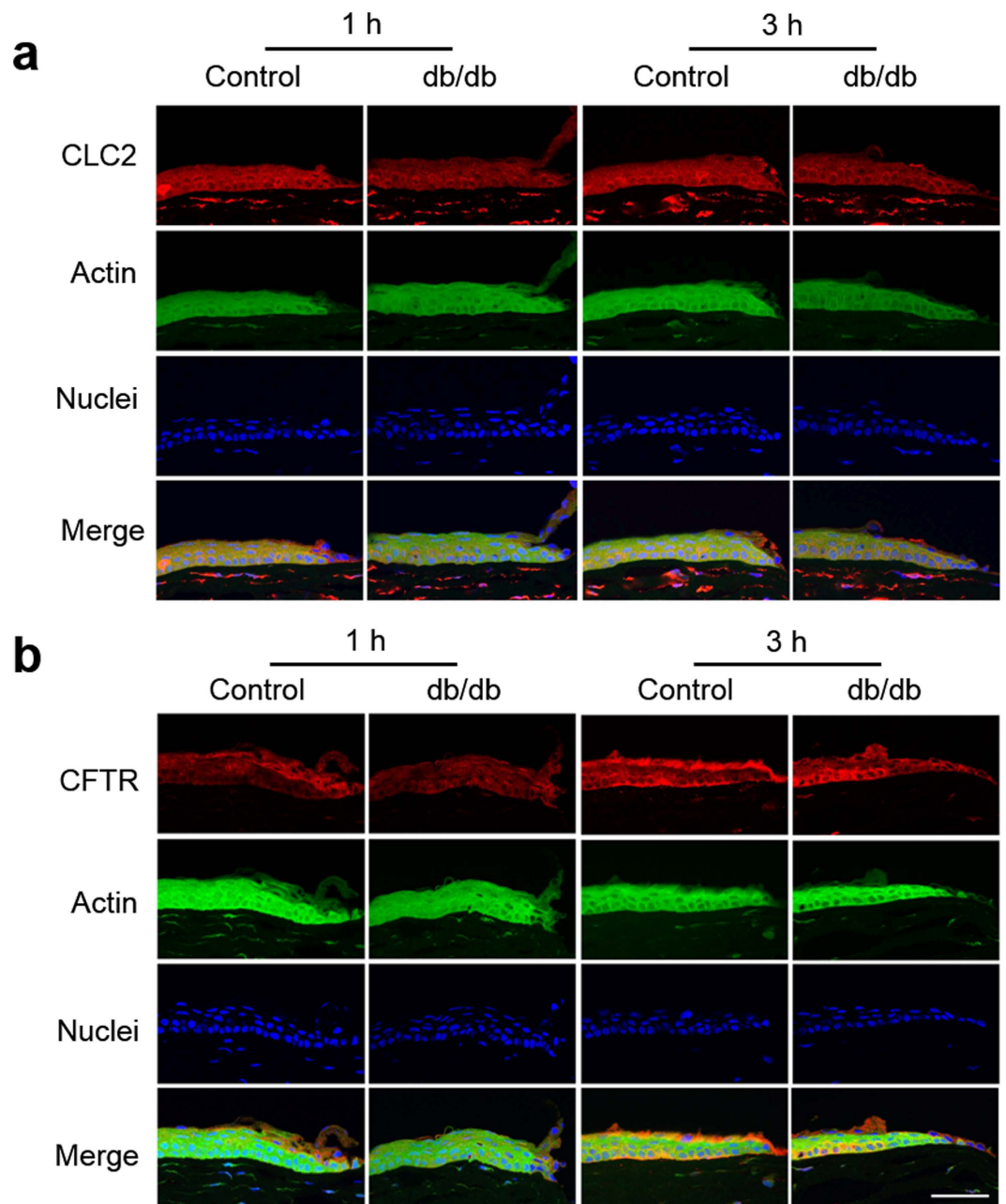


**Figure 5. Decreased expression of ion channels CLC2 and CFTR in the diabetic corneal epithelium.**

Genetic knockout db/db mice showed less CLC2 (a) and CFTR (b) compared to the control group 1 h and 3 h after wounding. The central, brightly-labeled portion is the corneal epithelium, with the stroma below and tear film above. The epithelial wound edges are to the right in each picture. Scale bar: 50  $\mu\text{m}$ .

proposed to be the major component of the wound electric currents in normal cornea wounds<sup>28,29</sup>. Both CLC2 and CFTR were expressed in the epithelial layers (Fig. 5). CLC2 showed weaker expression in the diabetic cornea wound than in the control cornea wound (Fig. 5a). Three hours after wounding, apical and basal expression of CFTR appeared to increase in the control cornea at the wound edge (Fig. 5b, 3 h post-wounding). These changes seemed to be weaker in the diabetic cornea at the same time. Therefore, fewer of these channels, and concomitantly less flux of  $\text{Cl}^-$  ions, can in part account for the decreased electric signal in diabetic corneas.

**Human corneal epithelial cells in high glucose showed impaired electrotaxis.** To determine whether high glucose impairs cell migration, we tested electrotaxis of CECs in EpiLife medium supplemented with 6 mM of D-glucose (total glucose (HG): 12 mM), and EpiLife medium supplemented with 6 mM mannitol to balance the osmolarity (mannitol control is 6 mM glucose plus 6 mM mannitol). In both conditions, cells responded to the applied EF of 100 mV/mm by migrating to the cathode (Fig. 6a,b). Compared to normal

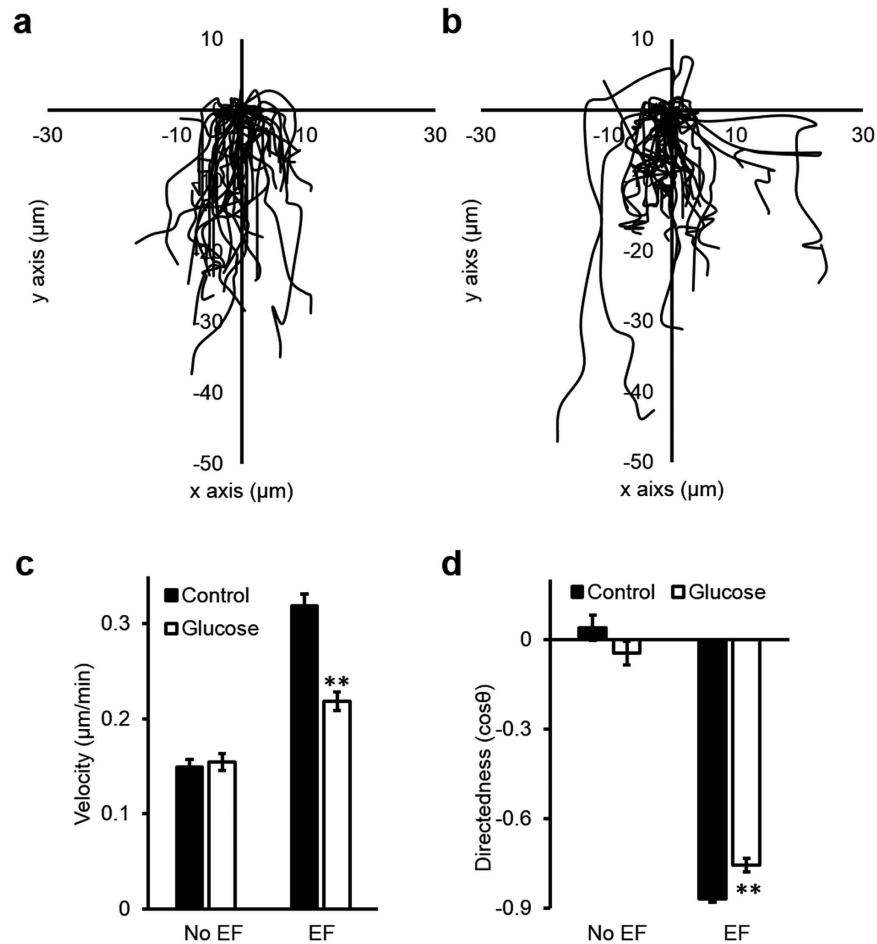


**Figure 6. High glucose impaired electrotaxis of human corneal epithelial cells (hCECs).** Cell tracks are shown with the position of each cell at the start of the experiment normalized to the origin. The cathode is at the bottom. (a) Trajectories of cells in mannitol control group (+6 mM mannitol). (b) Trajectories of cells in high glucose group (+6 mM D-glucose). (c) Velocity and (d) directedness of cells of control and high glucose groups respectively. Cells exposed to high glucose medium for 7 days showed significantly reduced speed and directedness. Data are mean  $\pm$  S.E.M. from 6 independent experiments. \*\* $p < 0.01$ , compared with control, Student  $t$ -test.

glucose, cells in high glucose migrated slower and with decreased directedness values ( $n = 6$ ,  $p < 0.01$ ; Fig. 6c,d; Movie S1).

## Discussion

In this study, we sought to determine whether diabetic wounds generate weaker electric signals relative to normal wounds, and if this in turn correlates with impaired wound healing in diabetes. We hypothesized that cell migration can be deregulated by the abnormal electric signals, leading to impaired healing. In three independent diabetes mouse models, vibrating probe measurements demonstrated that electric signals were significantly impaired at diabetic cornea wounds. Time lapse measurements revealed that the electric currents at diabetic corneas lost the normal rising and plateau phases which are associated with active (translocator-mediated) transport and pumping of ions via the cornea trans epithelial electric potential (TEP). The decreased diabetic electric signals correlated significantly with impaired wound healing. Expression of  $\text{Cl}^-$  channels CLC2 and CFTR appeared to be lower in diabetic corneas. Short-term high glucose exposure reduced electrotaxis of CECs, but not the electric current at cornea wounds.

Injury induces diverse biochemical and mechanical cues to instigate healing responses<sup>30,31</sup>. EFs at wounds may provide a powerful injury signal to mobilize and guide cells to heal wounds. Electric currents are present at wounds immediately after wounding and persist for hours, days and even weeks<sup>26,32–36</sup>. The negative pole (cathode) is located at the wound center relative to the surrounding intact tissues<sup>32,37</sup>. When stimulated with EFs of the strength that are measured *in vivo*, cells in culture show remarkable enhanced and directional migration towards the cathode<sup>19</sup>. EFs have therefore been proposed as a signal playing an important role in wound healing<sup>20,38</sup>. Neuropathy, micro-circulatory changes, altered growth factors and abnormal cytokine production play important roles in impaired wound healing in diabetes<sup>9,39–41</sup>. With data from three independent diabetic models, we provide the first set of experimental evidence that cornea wounds from diabetic animals had significantly impaired

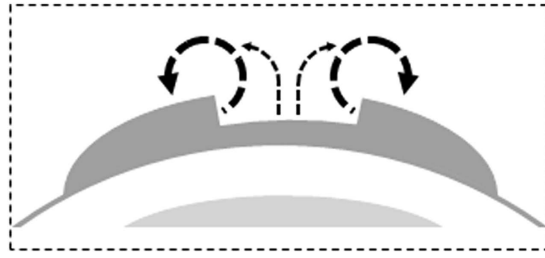


**Figure 7. Schematic showing possible path of circulating ion currents at a cornea wound.** We measured large outward currents at the wound edges, smaller outward currents at the wound center, and inward currents at the unwounded cornea outside the wound. The currents may therefore circulate out of the wound, flowing through the external solution, and in at the intact cornea, then flowing through the tissue to complete the circuit.

electric signals. Nuccitelli *et al.* found that wound EFs in older individuals were significantly smaller than those of younger adults<sup>42</sup>.

Here, quantitative analyses revealed significant correlations between the electric signals and wound healing rate, suggesting that weaker electric currents may contribute to the impaired diabetic healing (Fig. 4c). The correlation between weaker electric signals and the slower rate of wound healing is consistent with previous results showing that pharmacological manipulation of ion pumping to increase or decrease the corneal TEP and wound electric signal increased or decreased, respectively, the wound healing rate<sup>24</sup>. Our results provide experimental evidence supporting the use of electrical stimulation in treatment of refractory chronic wounds<sup>23,43</sup>. Similar to the dynamic time courses of production of cytokines and growth factors following wounding<sup>44</sup>, the electric signals following injury also have a dynamic time-course. In control mouse cornea wounds, we observed an initial leakage phase (L), a rising phase (R), and a plateau phase (P) (Fig. 2), as is also seen at cornea wounds in rats or human<sup>25,26</sup>. Cornea wounds from db/db, STZ- and HFD- induced diabetes all showed not only significantly smaller wound electric currents, but also lost the rising and plateau phases. We consider that the rising and plateau phases are likely due to an active response following injury. In some diabetic corneas, we even found inward currents. Similar results have been reported in *Pax6 (+/-)* mice<sup>45</sup>, where the presence of the electric signal rather than the direction of electric fields appeared to correlate with defective healing.

Acute exposure to high glucose for 3 hours did not alter the electric signal at the cornea wounds (Fig. S1), suggesting that short-term exposure to high glucose in our *ex vivo* model was different from the long-term diabetic condition in animal models. This is an important indicator that the defective electric signal at diabetic corneal wounds is not simply due to high glucose in the tear solution for a short period of time, and is likely due to one or more long-term and systemic effects. These may include altered transportation of ions in diabetic corneas, compromise in epithelial junctions, neuropathy, and abnormal metabolism in cells due to direct and/or indirect effects of long-term high glucose exposure. High glucose *in vitro* inhibited electrotaxis of CECs in a small applied EF (100 mV/mm), reducing both migration speed and directedness. Migration speed was down about 25%, but the directedness was reduced to a lesser extent (~10%) (Fig. 6). High glucose in diabetic tears thus may also compromise cell migration and contribute to impaired wound healing. The impaired wound healing (Fig. 4) therefore is likely due to a combination of defective electrotactic cell migration and impaired electric signaling. Their respective contributions warrant further investigation.

Our recent study suggested that the largest ion flux in cornea wounds is  $\text{Cl}^-$  flux and this ion flux plays a dominant role in generating the cornea wound current<sup>46</sup>. In order to elucidate the mechanisms of  $\text{Cl}^-$  transport, we studied CLC2 which is expressed abundantly and specifically in corneal epithelium<sup>29</sup>, and CFTR which is an anion transporter involved in airway epithelial wound repair<sup>47</sup>. Lower expression of CFTR and CLC2 seen in the epithelia of diabetic cornea wounds may contribute to the weaker diabetic cornea wound current. This data is consistent with the role of CFTR in the initial stages of wound healing *in vitro*<sup>47</sup>, and also suggests that  $\text{Cl}^-$  flux may regulate the impaired wound healing in diabetic patients. Based on the spatial profile of the wounded cornea (Fig. 1c), we postulate a possible simplified two-dimensional circuit of the electric current flow at the wound (Fig. 7). Thus, currents at the wound, especially at the wound edges but also inside the wound, flow outward and through the external solution. The 'circuit' is completed by inward current flow in the intact cornea around the wound.

In conclusion, cornea wounds in diabetes have abnormal electric signals which may contribute to impaired wound healing, possibly via cell electrotactic migration deregulation. Our data suggest a new player – electric signals – which are a potential therapeutic target in management of chronic and non-healing wounds. Management strategies targeting electric signals in combination with other well-established treatments may offer better outcomes for diabetic wounds.

## Methods

**Animals.** This study was carried out in accordance with the National Institutes of Health Guide for the Care and Use of Laboratory Animals. All procedures were approved by the University of California, Davis, Institutional Animal Care and Use Committee (protocols 16766 and 17876).

**Diabetic eyes.** Eight week old male BKS.Cg-Dock7m *+/+* Lepr db/J heterozygous (db/+), homozygous (db/db) mice and streptozotocin (STZ; 50 mg)-induced diabetic mice<sup>48</sup> and saline-injected control mice were



obtained from Jackson Laboratory. C57Bl/6J mice were placed on either a low fat (10% kcal; control) or high-fat (60% kcal) diet (Research Diets Inc., USA) at 5 weeks of age and were sustained for 24–26 weeks. The composition of these diets and the propensity of mice maintained on this high-fat diet to develop type 2 diabetes has been well described previously<sup>49</sup>. The blood glucose levels of the diabetic animals were measured before the ophthalmectomy using an Accu-Chek Aviva Plus blood glucose meter (Roche Diagnostics) (Table S1).

Experiments were performed on isolated whole eyes from male mice or male Sprague-Dawley rats. Animals were euthanized by inhalation of CO<sub>2</sub> and cervical dislocation. Eyes were removed using fine spring scissors (Fine Science Tools, USA) and placed in room temperature (RT) artificial tear solution (BSS+ intraocular irrigating solution; Alcon Laboratories, Inc., USA). Cornea wounds were made by scraping off approximately 1.5–2 mm<sup>2</sup> of epithelium with a 15° ophthalmologic scalpel (Beaver-Visitec, USA). Electric current density was measured with the vibrating probe (see next section *Vibrating probe*) starting at 5 min after wounding at the wound edge, as this is where the maximum wound electric currents are seen<sup>24</sup>. We also did time lapse measurements where we measured the wound edge current for several hours after wounding to establish a dynamic time-course of wound signal generation. To characterize the current density at different positions on the wounded cornea, we waited until 40 min after wounding, because the time lapse data showed that the electric signal reached maximum level 40–50 min after wounding (see Fig. 2a). For high glucose measurements, eyes were pre-incubated for 3 h in Medium 199 (M199) culture medium (Life Technologies, USA) supplemented with 24.4 mM glucose to give a final glucose concentration of 30 mM. Control eyes were pre-incubated in normal M199 (5.6 mM glucose) supplemented with 24.4 mM mannitol, to compensate for osmolality.

**Vibrating probe.** The vibrating probe technique for non-invasive measurement of endogenous electric current densities has been previously described in detail<sup>26</sup>. Briefly, the probe is an insulated stainless-steel microelectrode (World Precision Instruments, USA) with a platinum ball electroplated to the tip. The probe, mounted on a 3-dimensional micromanipulator (Line Tool Co., USA), is vibrated at high frequency (~200 Hz) in solution approximately 1 tip ball distance from the cornea surface by a piezoelectric bender. If an electric current is present due to ion flux, the charge on the platinum ball fluctuates in proportion to the size of the current. The probe is connected to a lock-in amplifier (SR530; Stanford Research Systems, USA) that locks on to the probe's specific frequency. The probe is calibrated with a current density of 1.5 μA/cm<sup>2</sup> at the start and end of experiments. The probe is vibrated in solution far from the cornea (>1 cm), where there is no electric current, to establish a baseline. The probe is then moved into measuring position close to the cornea (either intact unwounded cornea or wound center / wound edge; see Fig. 1a).

**Wound healing.** Wounds were made as in the previous section *Diabetic eyes*. Each eye was placed with the wound facing up in a 35 mm plastic dish containing an 800 μm nylon mesh (nitex mesh). Fluorescein dye was applied to the wound by placing one drop of artificial tear solution onto a Ful-Glo fluorescein sodium ophthalmic strip (Akron, Inc., USA) and then placing the drop onto the eye. Images were taken at 30× magnification using a Zeiss Lumar V12 microscope with AxioCam MRm camera and an EXFO X-cite 120 fluorescent illumination system. Eyes were incubated at 37 °C, 5% CO<sub>2</sub> in 6-well tissue culture plates with 6 ml of culture medium M199 (supplemented with 100 units of penicillin/streptomycin) in each well. Photographs were taken in fresh wounds and at 24, 30 and 48 h. Wound healing was assessed by measuring wound areas using Image J ([imagej.nih.gov/ij/](http://imagej.nih.gov/ij/)). Wound areas were normalized against the original fresh wound area and presented as percentage (%) of wound healing using the formula: ((original wound area – new wound area) ÷ (original wound area)) × 100.

For correlation of wound electric signal and wound healing, individual eyes (n = 4 for db/db and high-fat diet) were wounded and the wound edge electric current measured (for each eye, average of left and right wound edge currents). Then in the same eyes, wound healing was assessed. Data from each eye was plotted as normalized wound current vs wound healing (see Fig. 4c) and the Pearson correlation coefficient calculated (see section *Statistics* below). Each set of data (HFD and db/db) were normalized so that their maximum wound current was 1 μA/cm<sup>2</sup>, so they could be plotted on the same chart.

**Cells.** Human telomerase-immortalized CECs were a gift from the Christopher J. Murphy/Paul Russel laboratory, Departments of Ophthalmology and Surgical and Radiological Sciences, UC Davis. Cells were cultured in EpiLife medium (Life Technologies, USA) containing 6 mM D-glucose as normal control supplemented with EpiLife defined growth supplement (EDGS) and 1% penicillin/streptomycin (Life Technologies, USA). For high glucose experiments the medium was supplemented with additional 6 mM D-glucose (high glucose) or 6 mM D-mannitol (normal glucose balanced for osmolality) (Sigma-Aldrich, USA) for seven days.

**Electrotaxis.** Methods to study the migration of cells in applied EFs have been described in detail previously<sup>50</sup>. Briefly, a 22 × 10 mm electrotaxis chamber was coated with fibronectin-collagen mix (Athena Environmental Sciences, Inc., USA) for 5 min. Cells were seeded into the chamber for 30 min before the electrotaxis study began. An EF of 100 mV/mm was applied for 1 h via silver/silver chloride electrodes and agar bridges to prevent artefacts. Cell migration was recorded by time lapse phase contrast on an inverted microscope using Metamorph software. Cell directedness and speed were analyzed by Image J. Cosine  $\theta$ , defining cell directedness, is the average angle between the EF vector and a straight line connecting the start and end positions of all the cells which migrated in the EF. A  $\cos \theta$  value between –1 and 0 represents migration towards the cathode and 0 to +1 towards anode. Average  $\cos \theta$  of near 0 indicates random cell migration with no directionality. Velocity is accumulated distance migrated divided by time.

**Immunofluorescence.** Control and db/db mouse corneas with wounds were fixed in 4% paraformaldehyde for 2 h and then immersed in 10% and 30% sucrose solution, successively, for dehydration. Cryosections (8 μm thick) were fixed in cold acetone and permeabilized in 0.2% Triton X-100. After blocking with buffer containing 5%

donkey serum (Sigma, USA) with 1% BSA in 0.1% Triton X-100 PBS for 1 h, sections were incubated overnight with primary antibodies against chloride channel 2 (CLC2) (1:100; Santa Cruz Biotechnology, USA) or cystic fibrosis transmembrane conductance regulator (CFTR) (1:100; Santa Cruz Biotechnology, USA) at 4°C. Sections were then incubated with Alexa Fluor 594 conjugated donkey anti-rabbit IgG (H+L) secondary antibody (1:200; Life Technologies, USA). Negative controls included no primary antibody or isotype-specific control antibodies along with secondary antibodies. Nuclei and cytoskeleton were labeled with DAPI (Life Technologies, USA) and fluorescein isothiocyanate conjugated phalloidin (Sigma, USA), respectively. Images were obtained using an Olympus FV1000 confocal microscope with a 40x oil objective from comparative experiments.

**Statistics.** Data analyses, graphs, and statistical calculations were made using Excel (Microsoft) and SPSS V16.0 (SPSS Inc.). Data are expressed as mean  $\pm$  standard error of the mean (S.E.M.) or mean  $\pm$  standard deviation (S.D.). Differences between mean values were compared using Student *t*-test. Differences were considered statistically significant if *p*-value < 0.05. The correlation study was performed by Pearson correlation test. A Pearson correlation coefficient (R) close to one shows a good correlation. The *p* value gives the significance of the correlation, *p* < 0.05 showing a significant correlation.

## References

1. WHO. *Global status report on noncommunicable diseases 2014*. (2014) Available at: <http://www.who.int/nmh/publications/ncd-status-report-2014/en/>. (Accessed: 12<sup>th</sup> April 2016).
2. Ramsey, S. D. *et al.* Incidence, outcomes, and cost of foot ulcers in patients with diabetes. *Diabetes Care*. **22**, 382–387 (1999).
3. Singer, A. J. & Clark, R. A. Cutaneous wound healing. *N Engl J Med*. **341**, 738–746 (1999).
4. Fonder, M. A. *et al.* Treating the chronic wound: A practical approach to the care of nonhealing wounds and wound care dressings. *J Am Acad Dermatol*. **58**, 185–206 (2008).
5. Luttj, G. A. Effects of diabetes on the eye. *Invest Ophthalmol Vis Sci*. **54**, ORSF81–87 (2013).
6. Wang, E., Gao, N., Yin, J. & Yu, F. S. Reduced innervation and delayed re-innervation after epithelial wounding in type 2 diabetic Goto-Kakizaki rats. *Am J Pathol*. **181**, 2058–2066 (2012).
7. Ewald, M. & Hammersmith, K. M. Review of diagnosis and management of recurrent erosion syndrome. *Curr Opin Ophthalmol*. **20**, 287–291 (2009).
8. Rafahi, H., El-Osta, A. & Karagiannis, T. C. Genetic and epigenetic events in diabetic wound healing. *Int Wound J*. **8**, 12–21 (2011).
9. Blakytyn, R. & Jude, E. The molecular biology of chronic wounds and delayed healing in diabetes. *Diabet Med*. **23**, 594–608 (2006).
10. Du Bois-Reymond, E. *Untersuchungen uber thierische Electricitat, Zweiter Band, Zweite Abtheilung (Erste Lieferung)*. (Georg Reimer, 1860).
11. Klyce, S. D. Electrical profiles in the corneal epithelium. *J Physiol*. **226**, 407–429 (1972).
12. Song, B., Zhao, M., Forrester, J. V. & McCaig, C. D. Electrical cues regulate the orientation and frequency of cell division and the rate of wound healing *in vivo*. *Proc Natl Acad Sci USA* **99**, 13577–13582 (2002).
13. Chiang, M., Robinson, K. R. & Vanable, J. W. Jr. Electrical fields in the vicinity of epithelial wounds in the isolated bovine eye. *Exp Eye Res*. **54**, 999–1003 (1992).
14. Nuccitelli, R. A role for endogenous electric fields in wound healing. *Curr Top Dev Biol*. **58**, 1–26 (2003).
15. Sta Iglesia, D. D. & Vanable, J. W. Jr. Endogenous lateral electric fields around bovine corneal lesions are necessary for and can enhance normal rates of wound healing. *Wound Repair Regen*. **6**, 531–542 (1998).
16. Levin, M. H. & Verkman, A. S. Aquaporins and CFTR in ocular epithelial fluid transport. *J Membr Biol*. **210**, 105–115 (2006).
17. Chi, C. & Trinkaus-Randall, V. New insights in wound response and repair of epithelium. *J Cell Physiol*. **228**, 925–929 (2013).
18. Zhao, M., Agius-Fernandez, A., Forrester, J. V. & McCaig, C. D. Orientation and directed migration of cultured corneal epithelial cells in small electric fields are serum dependent. *J Cell Sci*. **109** (Pt 6), 1405–1414 (1996).
19. Nishimura, K. Y., Isseroff, R. R. & Nuccitelli, R. Human keratinocytes migrate to the negative pole in direct current electric fields comparable to those measured in mammalian wounds. *J Cell Sci*. **109** (Pt 1), 199–207 (1996).
20. Zhao, M. *et al.* Electrical signals control wound healing through phosphatidylinositol-3-OH kinase-gamma and PTEN. *Nature*. **442**, 457–460 (2006).
21. Aaron, R. K., Ciombor, D. M. & Simon, B. J. Treatment of nonunions with electric and electromagnetic fields. *Clin Orthop Relat Res*. **419**, 21–29 (2004).
22. Junger, M. *et al.* Local therapy and treatment costs of chronic, venous leg ulcers with electrical stimulation (Dermapulse): a prospective, placebo controlled, double blind trial. *Wound Repair Regen*. **16**, 480–487 (2008).
23. Herberger, K. *et al.* Effectiveness, Tolerability, and Safety of Electrical Stimulation of Wounds With an Electrical Stimulation Device: Results of a Retrospective Register Study. *Wounds—a Compendium of Clinical Research and Practice*. **24**, 76–84 (2012).
24. Reid, B., Song, B., McCaig, C. D. & Zhao, M. Wound healing in rat cornea: the role of electric currents. *FASEB J*. **19**, 379–386 (2005).
25. Reid, B., Graue-Hernandez, E. O., Mannis, M. J. & Zhao, M. Modulating endogenous electric currents in human corneal wounds—a novel approach of bioelectric stimulation without electrodes. *Cornea*. **30**, 338–343 (2011).
26. Reid, B., Nuccitelli, R. & Zhao, M. Non-invasive measurement of bioelectric currents with a vibrating probe. *Nat Protoc*. **2**, 661–669 (2007).
27. Sen, D. K. & Sarin, G. S. Tear glucose levels in normal people and in diabetic patients. *Br J Ophthalmol*. **64**, 693–695 (1980).
28. Vieira, A. C. *et al.* Ionic components of electric current at rat corneal wounds. *PLoS one*. **6**, e17411 (2011).
29. Cao, L. *et al.* Chloride channels and transporters in human corneal epithelium. *Exp Eye Res*. **90**, 771–779 (2010).
30. Fu, X. & Li, H. Mesenchymal stem cells and skin wound repair and regeneration: possibilities and questions. *Cell Tissue Res*. **335**, 317–321 (2009).
31. Gurtner, G. C., Werner, S., Barrandon, Y. & Longaker, M. T. Wound repair and regeneration. *Nature*. **453**, 314–321 (2008).
32. Mukerjee, E. V. *et al.* Microneedle array for measuring wound generated electric fields. *Conf Proc IEEE Eng Med Biol Soc*. **1**, 4326–4328 (2006).
33. Sta Iglesia, D. D., Cragoe, E. J. Jr. & Vanable, J. W. Jr. Electric field strength and epithelization in the newt (*Notophthalmus viridescens*). *J Exp Zool*. **274**, 56–62 (1996).
34. Vanable, J. W. Jr. *Intregumentary potentials and wound healing*. (Alan R. Liss, 1989).
35. Foulds, I. S. & Barker, A. T. Human skin battery potentials and their possible role in wound healing. *Br J Dermatol*. **109**, 515–522 (1983).
36. Illingworth, C. M. & Barker, A. T. Measurement of electrical currents emerging during the regeneration of amputated finger tips in children. *Clinical Physics and Physiological Measurement*. **1**, 87 (1980).
37. Barker, A. T., Jaffe, L. F. & Vanable, J. W. Jr. The glabrous epidermis of cavies contains a powerful battery. *Am J Physiol*. **242**, R358–366 (1982).
38. Reid, B., Song, B. & Zhao, M. Electric currents in *Xenopus* tadpole tail regeneration. *Dev Biol*. **335**, 198–207 (2009).

39. Barsun, A., Sen, S., Palmieri, T. L. & Greenhalgh, D. G. A ten-year review of lower extremity burns in diabetics: small burns that lead to major problems. *J Burn Care Res.* **34**, 255–260 (2013).
40. Falanga, V. Wound healing and its impairment in the diabetic foot. *Lancet.* **366**, 1736–1743 (2005).
41. Bettahi, I. *et al.* Genome-wide transcriptional analysis of differentially expressed genes in diabetic, healing corneal epithelial cells: hyperglycemia-suppressed TGFbeta3 expression contributes to the delay of epithelial wound healing in diabetic corneas. *Diabetes.* **63**, 715–727 (2014).
42. Nuccitelli, R. *et al.* The electric field near human skin wounds declines with age and provides a non-invasive indicator of wound healing. *Wound repair and regeneration : official publication of the Wound Healing Society [and] the European Tissue Repair Society.* **19**, 645–655 (2011).
43. Schaum, K. D. Decision on national coverage of electromagnetic therapy for wounds. *Adv Skin Wound Care.* **17**, 316–317 (2004).
44. Barrientos, S. *et al.* Growth factors and cytokines in wound healing. *Wound Repair Regen.* **16**, 585–601 (2008).
45. Kucerova, R. *et al.* The role of electrical signals in murine corneal wound re-epithelialization. *J Cell Physiol.* **226**, 1544–1553 (2011).
46. Reid, B. *et al.* Specific ion fluxes generate cornea wound electric currents. *Commun Integr Biol.* **4**, 462–465 (2011).
47. Schiller, K. R., Maniak, P. J. & Grady, S. M. Cystic fibrosis transmembrane conductance regulator is involved in airway epithelial wound repair. *American Journal of Physiology - Cell Physiology.* **299**, C912–C921 (2010).
48. Wang, Z. & Gleichmann, H. GLUT2 in pancreatic islets: crucial target molecule in diabetes induced with multiple low doses of streptozotocin in mice. *Diabetes.* **47**, 50–56 (1998).
49. Winzell, M. S. & Ahren, B. The high-fat diet-fed mouse: a model for studying mechanisms and treatment of impaired glucose tolerance and type 2 diabetes. *Diabetes.* **53** Suppl 3, S215–219 (2004).
50. Tai, G., Reid, B., Cao, L. & Zhao, M. Electrotaxis and wound healing: experimental methods to study electric fields as a directional signal for cell migration. *Methods Mol Biol.* **571**, 77–97 (2009).

## Acknowledgements

This work was supported by NIH EY019101 to M.Z. This study was supported in part by an Unrestricted Grant from Research to Prevent Blindness, Inc., and an NEI core grant. Y.S. is supported by a fellowship from the China Scholarship Council. F.F. is supported by Fundação para a Ciência e Tecnologia (FCT) grant SFRH/BD/87256/2012. M.F.N. is supported by NIH HL098200 and HL121059. We thank Dr. James Jester (UC Irvine) for the generous gift of hTCEpi cells. We are grateful to Bradley Shibata and Dr. Paul Fitzgerald, Dept. of Cell Biology and Human Anatomy, UC Davis, for help with cornea histology (NEI Core facilities Grant P30 EY012576, PI, John S Werner), and Madeline Nieves, Dept. of Pharmacology, UC Davis, for technical support. We also thank Dr. Vijay Raghunathan (Surgical and Radiological Sciences, UC Davis) for help with cell culture and imaging. We are also grateful to Dr. Rivkah Isseroff and Michelle So (Dermatology, UC Davis) for helpful discussions and initial tissue samples.

## Author Contributions

Y.S., T.P., B.R. and F.F. performed the experiments and acquired the data, M.F.N. provided LFD and HFD fed mice and contributed to the revision of the manuscript, Q.Z. provided some financial support and participated in analysis and interpretation of data. J.L. contributed to the revision of the manuscript and analysis of data. M.Z., B.R. and Y.S. conceived and designed the study. Y.S., B.R. and M.Z. wrote the manuscript.

## Additional Information

**Supplementary information** accompanies this paper at <http://www.nature.com/srep>

**Competing financial interests:** The authors declare no competing financial interests.

**How to cite this article:** Shen, Y. *et al.* Diabetic cornea wounds produce significantly weaker electric signals that may contribute to impaired healing. *Sci. Rep.* **6**, 26525; doi: 10.1038/srep26525 (2016).



This work is licensed under a Creative Commons Attribution-NonCommercial-ShareAlike 4.0 International License. The images or other third party material in this article are included in the article's Creative Commons license, unless indicated otherwise in the credit line; if the material is not included under the Creative Commons license, users will need to obtain permission from the license holder to reproduce the material. To view a copy of this license, visit <http://creativecommons.org/licenses/by-nc-sa/4.0/>